Coherent Structures in the Inner Layer of Wall Turbulence under the Spatial Restriction

SHIGEO MARUYAMA and HIROAKI TANAKA
Department of Mechanical Engineering
The University of Tokyo
Hongo 7-3-1
Bunkyo-ku, Tokyo 113, Japan

ABSTRACT

The shear flow between a stationary flat plate and a moving plate with an array of tall fences, in which the systematic hot-film measurements have been carried out by Maruyama and Tanaka (1987a), is visualized by the unconventional but carefully examined aluminium-powder-suspension method. The streaky structures visualized are compared with those in the plane turbulent Couette flow. The sound structure of the fully-developed wall turbulence is demonstrated in the inner layer which is spatially restricted by the fence-tips, which pass at $y^+ = 49$ above the stationary plate. Furthermore, observed features of the visualized inner-layer structure under severer spatial restrictions agree qualitatively well with the previously introduced flow-regime map in the (h^+, p^+)-plane. These results clearly demonstrate the toughness and the self-sustenance of the inner-layer structure. In addition, the streamwise length-scale and celerity distributions of the visualized streaks, which are associated with the vortical motions, are obtained for the spatially restricted flows as well as for the plane turbulent Couette flows.

1. INTRODUCTION

Coherent structures characterized by low-speed streaks, streamwise vortices, and/or burstings, which are observed in the inner layer of wall turbulence, have been demonstrated to be responsible for a large part of the turbulence-energy production near the wall. Experimental works carried out in the last two decades have contributed to the knowledge about various aspects of the inner-layer structure (e.g., see Cantwell 1981; Hirata et al. 1982). However, the interaction between the inner and outer layers and its physical significance are still an open question.

Maruyama and Tanaka (1987a), which is hereafter referred to as M&T, queried whether the inner-layer structure was primarily dependent on the outer-layer structure, or rather self-sustaining. They tried to artificially change the structure of the outer layer, rather than simply observing the inner-layer structure of undisturbed fully-developed wall turbulence. To this end, a particular type of Couette flow was constructed; the flow between a flat plate and a moving parallel plate with an array of repeated tall fences, where the effect of spatial restriction imposed by the moving fences on the inner-layer structure of the flat plate boundary-layer was investigated. Through the hot-film measurements, it was found that the inner-layer structure could be well maintained even when the tips of the

successive fences were passing at the distance of $y^+ = 45$ from the wall. Furthermore, their parametric studies resulted in the flow-regime map in the (h^+, p^+)-plane, which is reproduced in Figure 1. This diagram represents the effects of the dimensionless streamwise pitch of the moving fences, p^+, and the dimensionless distance between the flat plate and the tips of the fences, h^+ (see Figure 2). Each symbol in Figure 1 denotes the experimental conditions of p^+ and h^+, under which the state of the flow is distinguished as 'fully turbulent', 'transitional', or 'laminar-like', based upon the mean velocity profile and the spectrum of velocity fluctuations. M&T concluded that the inner-layer structure has tough and self-sustaining physical mechanism and is hardly influenced by the outer-layer disturbances, provided that the spatial extent of about 45 ν/u^* from the wall and the wall shear-stress are ensured.

Later, Maruyama and Tanaka (1987b) extended the p^+-range of the experiments to very large p^+ values, which were estimated to be much larger than the streamwise length of the coherent structures, and discussed the recovery process of turbulence after the very severe spatial restriction (including the case of $h^+ = 0$). As a result, no conspicuous structural change was found in the inner-layer structure responding to the change of the outer-layer structure, and, hence, the toughness of the inner-layer structure was again confirmed.

In the present paper, the flow-visualization study of the inner-layer coherent-structures under the spatial restriction is undertaken in order to supplement the experimental evidence for the self-sustenance of the coherent structures. Among the experiments by M&T, those labelled 'F236' (see Figure 1) are further studied by using the hydrogen-bubble method as well as the aluminium-powder-suspension method. The photographic records, which are obtained under the several conditions of the F236 series and

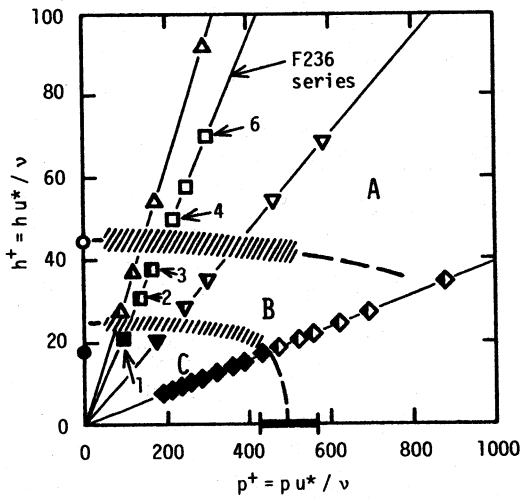

FIGURE 1. Flow-regime map in the (h^+, p^+)-plane reproduced from Maruyama and Tanaka (1987a): open symbols in region A are 'fully turbulent'; half-solid symbols in region B 'transitional'; and solid symbols in region C 'laminar-like'; △, F315 series (h = 20 mm and p = 63.5 mm); □, F236 (15 mm and 63.5 mm); ▽, F118 (15 mm and 127 mm); ◇, F039 (5 mm and 127 mm). Numbered symbols in F236 series denote the runs presently reexamined by the flow visualizations.

TABLE 1. Experimental conditions of F236 series in M&T (h = 15 mm and p = 63.5 mm) and turbulent Couette flows. Here, for the Couette flows (C075 and C100), h and U_c denote half the distance between two plates and the half the moving plate velocity, respectively.

Run No.	h^+	p^+	U_c (mm/s)	u* (mm/s)	Re_h hU_c/ν	ν/u^* (mm)	ν/u^{*2} (ms)	Distinction by M&T
F236:1	20.7	87.8	35.2	1.61	454	0.723	450	laminar-like
F236:2	31.5	133	48.9	2.35	654	0.477	203	transitional
F236:3	37.2	158	60.0	2.86	782	0.403	141	transitional
F236:4	49.3	209	72.3	3.65	977	0.304	83.5	fully turbulent
F236:6	71.0	300	99.7	5.25	1350	0.211	40.3	fully turbulent
C075	60.8	-	37.7	2.54	903	0.329	130	-
C100	77.9	-	50.5	3.30	1190	0.257	77.8	-

those of the turbulent Couette flows, are carefully analyzed in comparison with the flow-regime map in the (h^+, p^+)-plane shown in Figure 1. The streaks visualized by the aluminium-powder-suspension method are found to be associated with the streamwise vortical structures. The streamwise length and the celerity of the visualized streaks are roughly estimated for the 'fully-turbulent' runs among the F236 series and the turbulent Couette flows.

2. EXPERIMENTAL APPARATUS AND PROCEDURE

Flow visualization study has been made for the flows of F236 series, of which experimental conditions are summarized in Table 1. The dimensionless distance h^+ between the upper flat-plate and the tips of the fences, and the dimensionless pitch of the fences p^+ are changed with the velocity of the moving plate with the fences U_c (also see Figure 2). During the present experiments of flow visualization, differences in values of these parameters from those for the original flows in M&T are typically less than ± 1 %. Note that each flow in the F236 series in Table 1 is classified

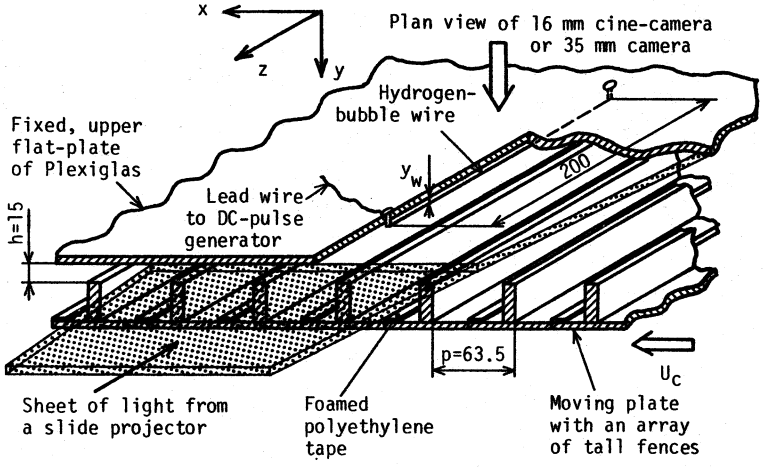

FIGURE 2. Sketch of the flow-visualization setup. Dimensions in mm.

into either 'laminar-like', 'transitional', or 'fully turbulent' by M&T.

The experimental apparatus for the F236 series in M&T is used with some modification for the measuring station. The measuring station with the flow-visualization setup is sketched in Figure 2. The hydrogen-bubble wire (a 50 μm tungsten wire) is stretched in the spanwise direction at certain vertical positions of y_w (3.4 or 3.8 mm) parallel to the fixed, upper flat-plate. About 4 grams of aluminium powder and a few drops of liquid detergent are added to the 600 liter of working water in the test tank. Each piece of the aluminium powder is a thin flake, with a typical diameter less than 50 μm and a thickness a few microns. The dilute suspension of aluminium flakes as well as the hydrogen bubbles are illuminated by a horizontal sheet of light from a slide-projector. A 16 mm cine-camera or a 35 mm camera is mounted about 950 mm above the flat plate for a plan view. An end view normal to the flow direction can be obtained through the clear Plexiglas tank-wall. The motion pictures are analyzed on a film-motion analyzer which is equipped with a digitizer interfaced with a mini-computer.

Hot-film measurements are also carried out to examine the velocity and turbulent intensity profiles and to determine the basic flow parameters for the Couette flows. Each tall fence element in Figure 2 is overturned to constitute a moving flat plate. The distance H between this moving plate and the fixed flat plate is kept as 40 mm. The resultant aspect ratio (the spanwise width to the distance H) is 15, while the entrance length 31H downstream of a coarse screen attached at the inlet of the fixed flat plate. The velocity measurements by the hot-film anemometer are carried out with the measuring station used by M&T, employing the same measuring procedure. Experimental conditions for these velocity measurements are also included in Table 1. The flow-visualization setup for the Couette flows is identical with that for the F236 series.

3. RESULTS AND DISCUSSIONS

3.1 Hot-Film Measurements for Turbulent Couette Flows

Figure 3(a) shows the mean velocity profiles for Couette flows together with the data of F236:4 and those at Re_h = 9500 by El Telbany and Reynolds (1982). The friction velocity is obtained from the slope of the linear velocity profiles close to the wall. The measured mean velocity at the center between the two plates agrees within ± 7 % with half the moving wall velocity U_c. Due to the imperfect adjustment of the flow-inlet condition, a small streamwise pressure gradient seems to exist, which is, however, negligibly small with respect to the realization of the standard structure of wall turbulence to be observed (see El Telbany and Reynolds 1980). The measured turbulent intensity profiles are shown in Figure 3(b), where the data of F236:4 run represents the profile of the standard wall turbulence in the inner layer. Though the velocity measurements include a considerable uncertainty of ± 5 % (20:1 odds), it is confirmed that the turbulent Couette flows presently realized should be of standard nature.

3.2 Aluminium-Powder-Suspension Method for the Inner-Layer Structure

The thin-flake-suspension method, such as aluminium powder and titanium-dioxide-coated mica platelets, has the advantage over other tracer methods using dye or hydrogen bubbles, because it gives the instantaneous spatial distribution of the turbulence structures. In transitional boundary

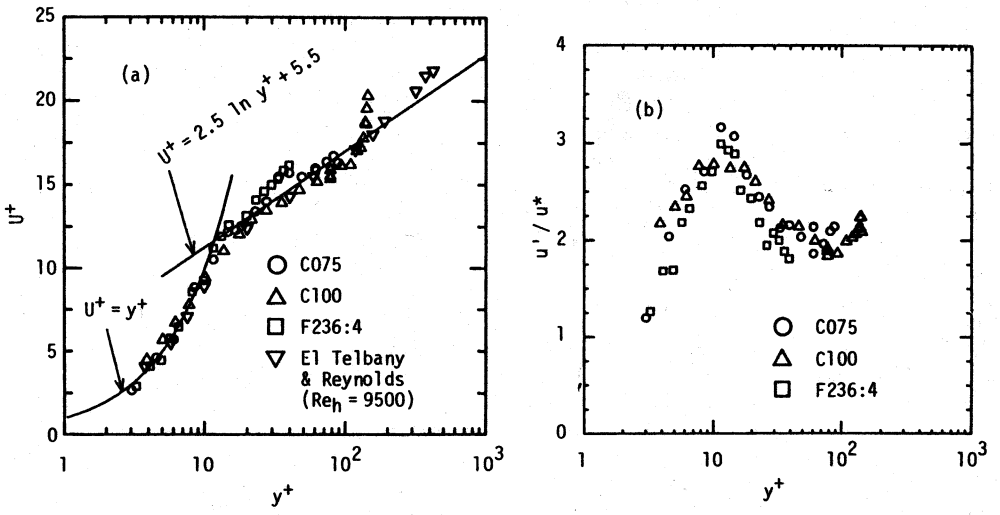

FIGURE 3. Hot-film measurements for turbulent Couette flows: (a) mean velocity profiles; (b) turbulent intensity profiles.

layers, this method has been employed to observe the turbulent spots, (e.g., Cantwell et al. 1978, Carlson et al. 1982, and Alavyoon et al. 1986). However, visualizations of the inner-layer structure of fully-developed wall turbulence have only been reported by Cantwell et al. (1978). They used a very dense suspension (about 500 times as dense as present) of aluminium powder and observed the streamwise streaks, which they speculated to represent the streamwise vortices.

With the present dilute suspension, streamwise bright streaks of the aluminium flakes are observed when illuminated in the plane parallel to the

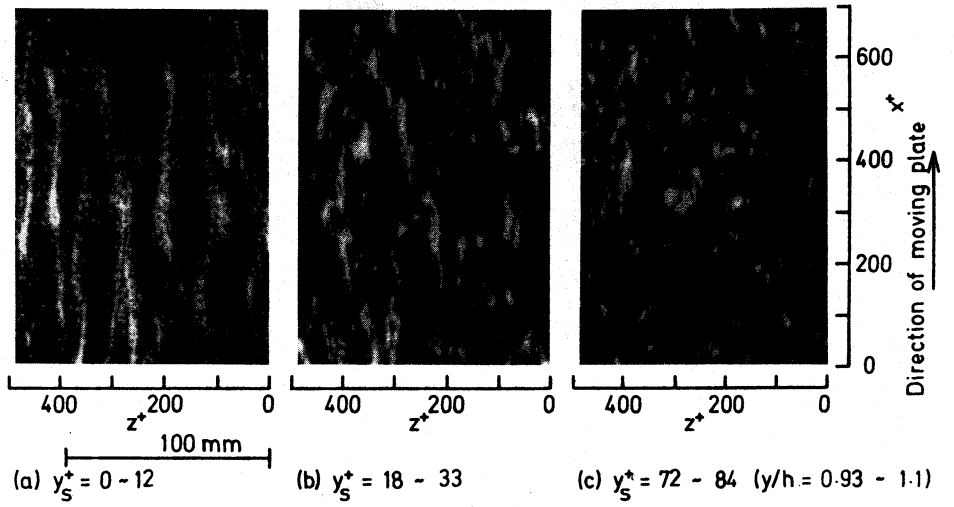

FIGURE 4. Examples of the aluminium-powder-suspension (APS) visualization in the Couette flow (C100) with the sheet of light at various distances from the fixed plate. See Figure 2 for the coordinate system.

wall from the spanwise side. Here, when the flow is illuminated in the same plane from the downstream direction, the streaks are not observed. Figure 4 shows typical examples of these streaks in the plane turbulent Couette flow with a sheet of light at various distances from the wall. Note that the depth of the sheet of light is about 12 wall units in Figure 4. When the near wall region is illuminated, very clear streamwise streaks are seen as shown in Figure 4(a). As the distance from the wall is increased, streamwise length of the streaks generally becomes shorter. As shown in Figure 4(c), the view is no longer recognized as the streamwise streaks at the center of the two plates.

Figure 5 is an example of simultaneous visualization in the Couette flow by the aluminium-powder-suspension method (APS method) and the hydrogen-bubble method (HB method). It is observed that a bright streak of aluminium flakes corresponds well to a low-speed streak visualized by the HB method. This correspondence is much more clearly visible in the motion pictures. With a careful observation of the motion pictures, however, it is found that a spanwise position of a bright streak's ridge does not coincide precisely with the position of the instantaneous valley of H_2 time lines, but is slightly biased toward opposite to the light-source side. Hence, two different color (Red and Green) lights from the both sides of the flow field are simultaneously used. A sketch of the color photograph obtained is shown in Figure 6, together with an imaginary end-view of the hydrogen-bubbles which is constructed by referring to simultaneous plan and end views of the hydrogen bubbles shown in figure 7. A low-speed streak visualized by the HB method accompanies both Red and Green bright streaks by which the ridge of the low-speed streaks is clearly observed. On the other hand, Figure 7, which is one of the successive photographic records obtained by two cameras simultaneously, apparently demonstrates that the low-speed regions in plan view are related to the low-momentum fluid

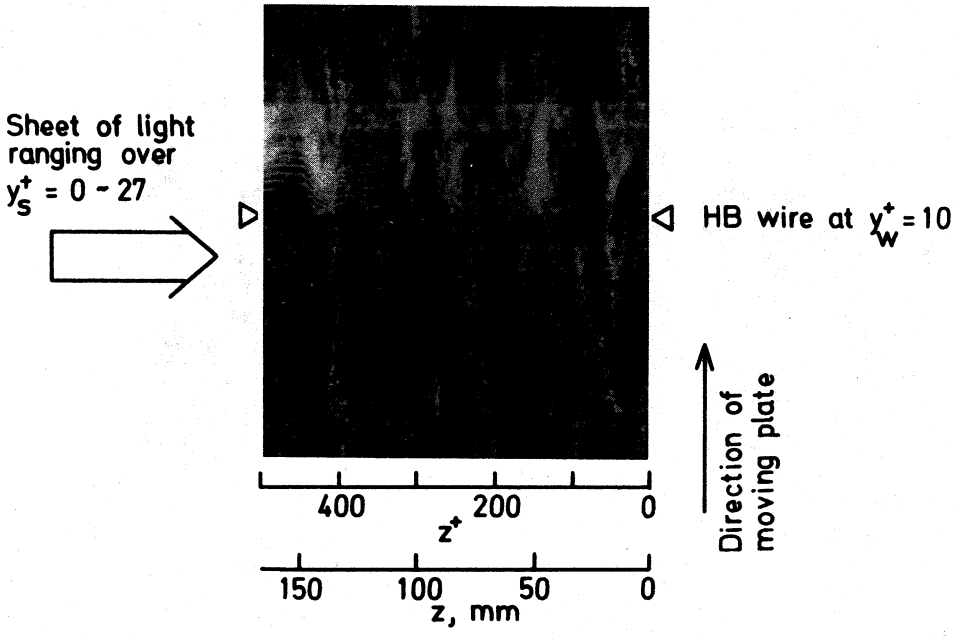

FIGURE 5. An example of simultaneous flow visualization in the Couette flow by the APS and HB methods (C075, Δt_{HB} = 0.12 s)

leaving away from the wall. This flow module is suspected to be caused by the streamwise vortices with their centers at $y^+ = 20 \sim 30$ (Blackwelder and Eckelmann 1979; Smith and Schwartz 1983; and Kasagi et al. 1986). Thus, the bright streak visualized by the APS method corresponds to the lifting-up region of this flow module.

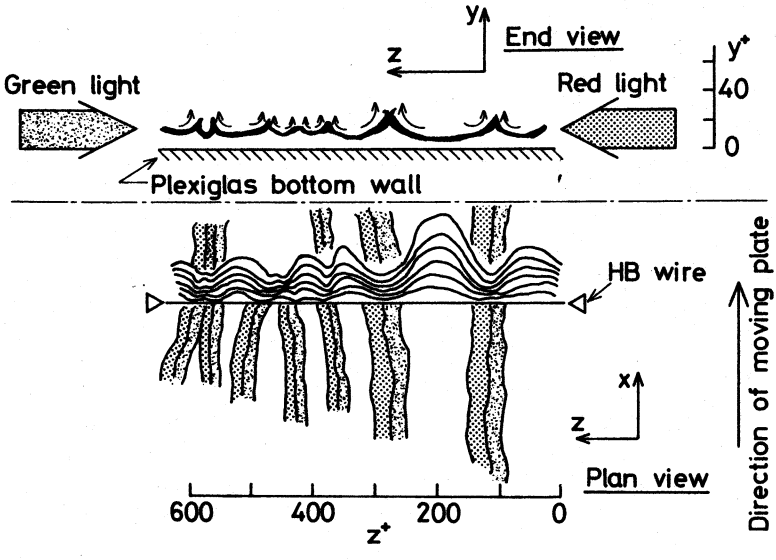

FIGURE 6. A sketch of the color photograph under the illumination simultaneously with two different color lights from the both sides of the flow field. Note that the plan view (x-z plane) is observed *through* the Plexiglas bottom wall. For the end view, the scale of y-direction is somewhat elongated.

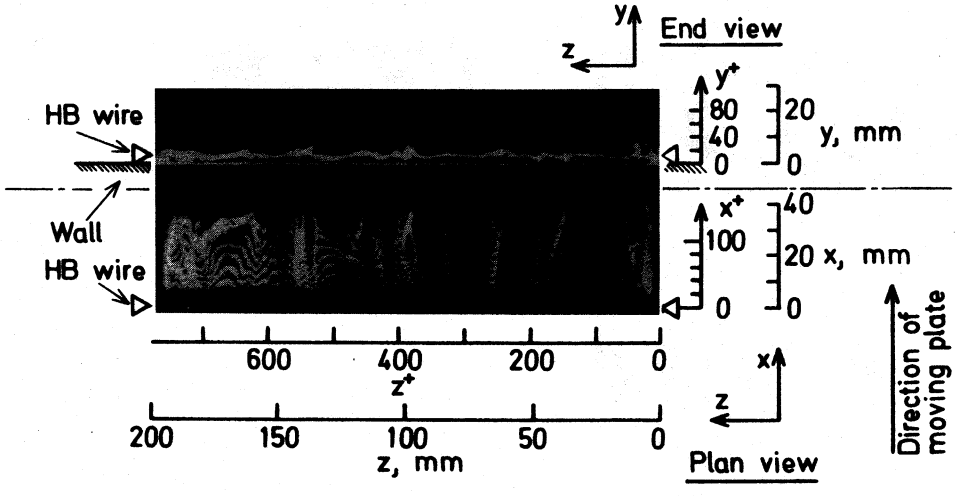

FIGURE 7. Simultaneous plan and end views of the hydrogen bubbles in the turbulent Couette flow (C100, $y_w^+ = 13$, $\Delta t_{HB} = 0.1$ s). Streamwise range of the illumination is the region where hydrogen bubbles are visible in the plan view.

According to a theoretical treatment of the motion of ellipsoidal particles in the uniform shear flow by Jeffery (1922), a thin disk spends most of its time near alignment with stream surfaces and flips over rapidly when at large angles to the flow. His theory was supported by a microscopic observation by Goldsmith and Mason (1962). Recently, Savaş (1985) introduced the further analysis of flow visualization using such flakes based on a stochastic treatment of Jeffery's solution and compared with the flow visualizations carried out for examples. If the vortical motion as shown in Figure 6 is assumed, flakes should align nearly with the curved arrows (showing the vortical motion in the end view). Hence, for example, the vortical module on the right-hand side of a low-speed streak in Figure 6 reflects the Green light to the Plexiglas bottom wall, through which the plan view is observed. Hereafter, we call these bright streaks visualized by the APS method as 'vortical streaks'.

3.3 The Inner-Layer Structure under the Spatial Restriction

The vortical streaks in the F236 series are visualized by the APS method and compared with those in the turbulent Couette flows. Examples of APS visualizations for the F236 series are shown in figure 8. The distance of the sheet of light from the wall y_s^+ is kept the same as in the case of the Couette flow shown in Figure 4(a). The illumination is made from only one side in the spanwise direction so that the one to one correspondence between the vortical streak and the low-speed streak is ensured. Pictures of F236:1 and F236:2 are slightly different from the others as well as the turbulent Couette flow shown in Figure 4(a) in their spanwise spacing of the

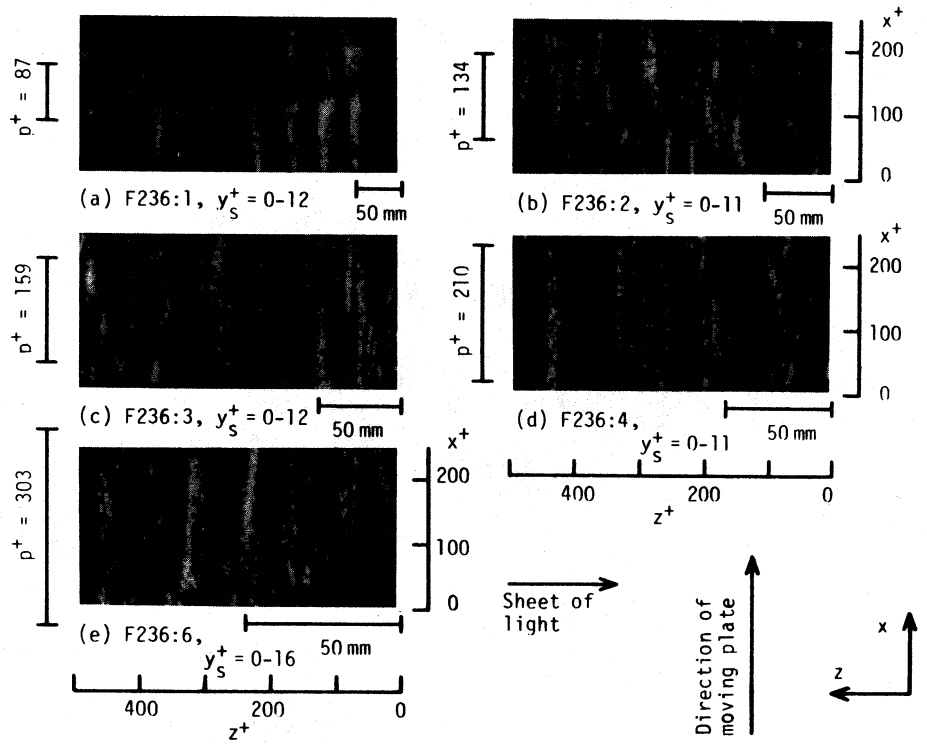

FIGURE 8. Examples of APS visualizations for the F236 series.

bright streaks.

For more quantitative comparison of the F236 series with the Couette flow, the motion pictures of the vortical streaks visualized by APS method and also of the low-speed streaks visualized by the HB method are carefully analyzed. For this, the APS and HB methods are employed independently under their best illumination conditions. In a frame of the motion picture of the HB visualization projected on the stop-motion analyzer, spanwise positions of low-speed streaks at a streamwise position slightly downstream of the hydrogen-bubble wire are determined with the following rule and are manually digitized and stored on the computer. The rule determining a low-speed streak is almost equivalent to the rules adopted by Smith and Metzler (1983) and Iritani et al. (1985). When low-speed peaks of successive time lines are observed for a given time interval, typically 6 ν/u^{*2}, it is marked as a low-speed streak. The sampling interval of the frames is determined typically as 6 ν/u^{*2}. In the case of the APS visualization, spanwise positions of the ridge of the bright streaks at a fixed streamwise position are digitized by the same method. When the streamwise length of a bright streak exceeds 100 ν/u^*, it is marked as a vortical streak.

The mean and the coefficient of variation of the spanwise spacings of the vortical streaks and the low-speed streaks are shown in Figure 9 for all the cases examined here. Also included are results of the two-dimensional channel flow by Iritani et al. (1985) and of the flat plate boundary-layer by Smith and Metzler (1983). Figure 10 summarizes the probability-density distributions of the spanwise spacings of the vortical streaks and the low-speed streaks. In Figure 10(a), the distribution in one of the 'fully-turbulent' runs (F236:4) is compared with those in the Couette flow and the channel flow by Iritani et al. (1985). The four distributions in Figure 10 (a) agree well. The distributions are well represented by the log-normal distributions as suggested by Nakagawa and Nezu (1981). Figure 10(b) shows the probability-density distributions for the whole F236 series. The distributions of the F236:4 and F236:6 are almost the same each other and quite similar to those of the turbulent Couette and channel flows. Hence, they can be recognized again as 'fully turbulent' in accordance with M&T (Table 1).

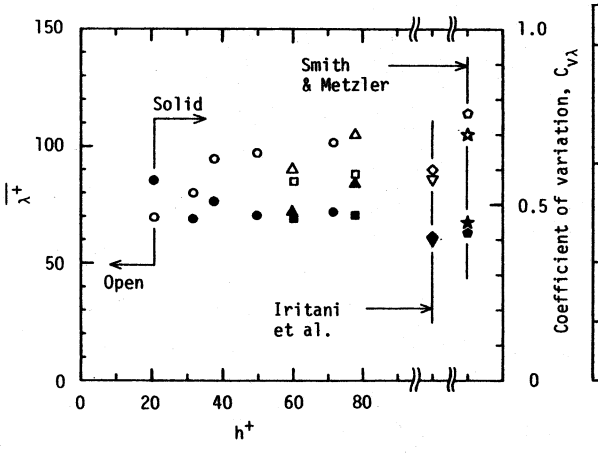

$\bar{\lambda}^+$	$C_{v\lambda}$	Run No. and Method		y_w^+ or y_s^+
○	●	F236:1 (h^+ = 20.7)	APS	0 - 12
○	●	F236:2 (h^+ = 31.7)	APS	0 - 11
○	●	F236:3 (h^+ = 37.6)	APS	0 - 12
○	●	F236:4 (h^+ = 49.7)	APS	0 - 11
○	●	F236:6 (h^+ = 71.5)	APS	0 - 16
△	▲	C075	APS	0 - 12
△	▲	C100	APS	0 - 12
□	■	C075	HB	10.2
□	■	C100	HB	13.2
▽	▼	Iritani et al.	HB	7.8
◇	◆	(Re_θ = 300)	HB	11.7
☆	★	Smith et al.	HB	10
⬠	⬟	(Re_θ = 2030)	HB	15

FIGURE 9. The mean and the coefficient of variation of the vortical streaks and low-speed streaks. Abscissa has no meaning for the data by Iritani et al. (1985) and Smith and Metzler (1983).

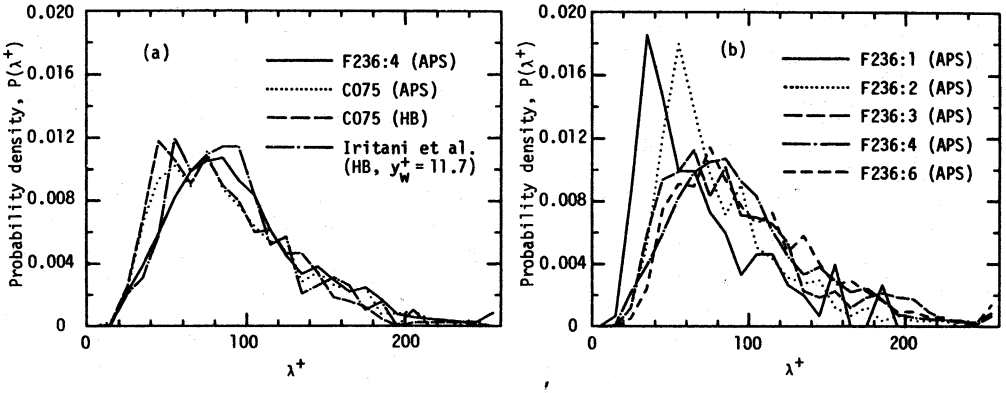

FIGURE 10. Probability-density distributions of the spanwise spacings of the vortical streaks and the low-speed streaks: (a) the F236:4 run, the Couette flow, and the channel flow by Iritani et al.; (b) F236 series.

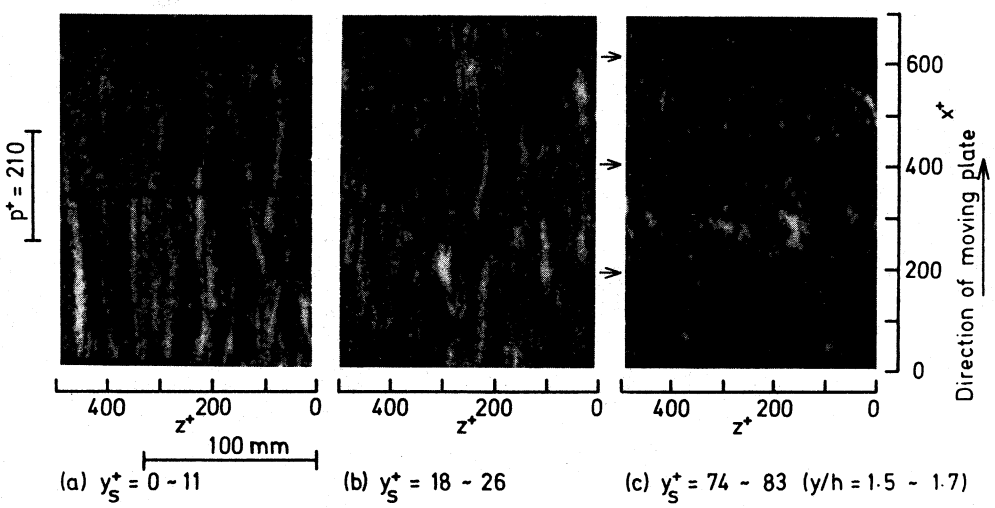

FIGURE 11. Examples of APS visualizations for the F236:4 run with the sheet of light at various distances from the wall. Small arrows in the left-hand side of (c) show instantaneous positions of the fences.

Figure 11 shows the examples of the APS visualization for one of the 'fully-turbulent' runs (F236:4) with the sheet of light at various distances from the wall. Flow structures observed in two near-wall regions, shown in Figures 11(a) and (b), seem to be very much similar to those in the Couette flow shown in Figures 4(a) and (b). Though the tips of the fences pass over the stationary wall at $y^+ = 49$, no appreciable effect is observed on the near-wall structure. In contrast, the structure in the region far from the wall shown in Figure 11(c) seems to be drastically changed by the passing fences, if compared with Figure 4(c). Note that the region in Figure 11(c) is located deep in the gap between the fences.

As shown in Figure 10, the M&T's 'transitional' F236:3 also agrees with the undisturbed standard flows in distributions of the spanwise spacing of the

vortical streaks. The 'transitional' F236:2 and the 'laminar-like' F236:1 are quite different from the fully turbulent flows. In these cases, the spanwise spacings are generally smaller than those in the fully turbulent flows. Furthermore, the larger probability at the most probable spacing suggests that the inner-layer structure under the very severe spatial restriction is more ordered than that of the fully turbulent flow. In the motion pictures, the vortical streaks appear only intermittently in the case of F236:1.

Some runs additional to the F236 series with more severer spatial restriction than that of F236:1 are visualized; for $h^+ = 20$ ($U_c = 31$ mm/s) and $h^+ = 18$ ($U_c = 25$ mm/s). Thirty successive photographs at a time interval of 10 s for each case are examined. In the former, the bright streaks have rarely appeared, while in the latter, no bright streaks have been observed. In the (h^+, p^+)-plane shown in Figure 1, these new experimental points locate slightly below the boundary between transitional and laminar-like.

3.4 Some Further Analyses for the 'Fully-Turbulent' Runs.

The probability-density distribution of the streamwise length-scale of the vortical streaks is obtained from the APS-visualization motion pictures. For each bright vortical streak detected, the coordinates of the streamwise edges are manually taken into the computer. When an edge is out of a frame, an image in a few frames forward or behind is used. In addition, the edges of a visualized bright streak are often difficult to identify. Thus, the length-scale distribution has a considerably large uncertainty. Figure 12 shows the results for the 'fully-turbulent' runs in the F236 series and the Couette flows. The distributions of the length-scale reaches 800 ν/u^* at most with the mean value of 300 to 400 ν/u^*. No difference is perceived between the 'fully-turbulent' runs of the F236 series and the turbulent Couette flows. It should be emphasized that in the case of the F236:4 run, the streamwise pitch of the fence-tips, which pass at $y^+ = 49$ above the stationary plate, is 210 ν/u^* which is much smaller than the mean streamwise length-scale of the streaks. Thus, a typical streak must always lie beyond two or three tips of the fences.

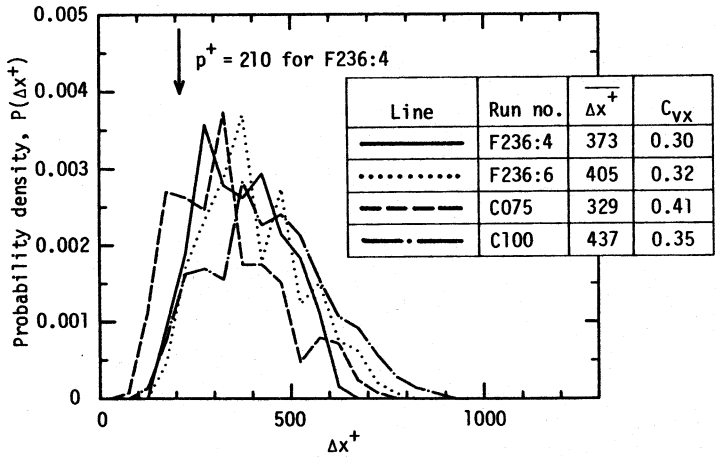

FIGURE 12. Probability-density distributions of the streamwise length-scale of the vortical streaks.

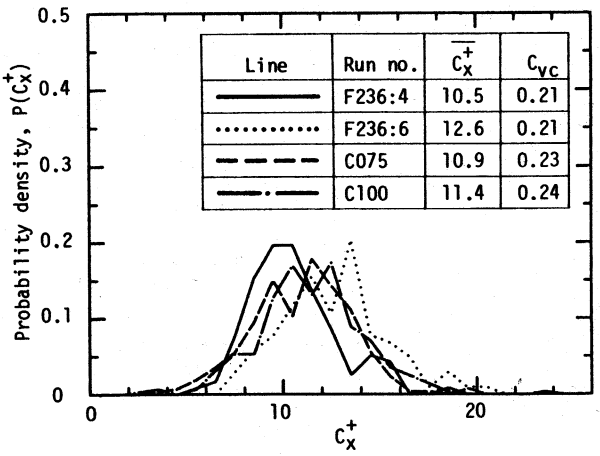

FIGURE 13. Probability-density distributions of the celerity of the vortical streaks.

Remarking a representative point in a streak, which is a mid point of the brightest portion, and advancing a given number of frames, it is possible to obtain the displacement over which the bright pattern travels during the time interval. With this time interval about 12 ν/u^{*2}, the distributions of the celerity of vortical streaks are obtained as shown in Figure 13. In spite of the considerable uncertainties involved in the data reduction, there seems no distinct difference between the distributions for the 'fully-turbulent' runs and those for the turbulent Couette flows. The mean celerity of the streaks of about 11 u* is comparable to the convection velocity of 12.1 u* of the velocity fluctuations in the viscous sublayer which has been obtained by the correlation method (Kreplin and Eckelmann 1979).

4. CONCLUSIONS

It is demonstrated that the aluminium-powder-suspension method is useful in visualizing the streamwise vortical structures in the inner layer of wall turbulence. When the inner layer is illuminated by a sheet of light in the plane parallel to the wall from the spanwise side, the bright streaks are observed. These streaks represent the lift-up motion of low-speed fluid from the wall caused by the vortical motion, and is in one to one correspondence with the low-speed streak visualized by the hydrogen-bubble method. Using this flow-visualization technique, the spatially restricted flows are compared with the fully-developed turbulent Couette flows; comparisons are made in distributions of the spanwise spacing, the streamwise length-scale, and the celerity of the bright streaks. As a result, it is found that the inner-layer structure under the spatial restriction with the fence-tips, 49 ν/u^* above the stationary plate, has the vortical structures similar to those in the standard wall turbulence. Furthermore, observed features of the vortical structures in the F236 series are consistent with the implication of the flow-regime map in the (h^+, p^+)-plane given by M&T. Thus, it is again demonstrated that the vortical structures in the inner layer are not influenced by the spatial restriction unless they are directly touched by the tips of the fences. In a general conclusion, the inner-layer coherent structure has tough and self-sustaining physical mechanism.

ACKNOWLEDGEMENT

The authors wish to thank Mr. Satoshi Dodo and Mr. Tsuyoshi Tamura for their help in the experiments and Professor Nobuhide Kasagi for his helpful comments and suggestions.

NOMENCLATURE

C_v Coefficient of variation, i.e., standard deviation divided by mean.
C_x Celerity of the vortical streak.
H Distance between the two plates for Couette flows.
h For F236 series, distance between the tips of the fences and the fixed flat plate. For Couette flows, half the distance between the two plates.
P( ) Probability density.
p Streamwise pitch of the moving fences.
Re_h Reynolds number defined as hU_c/ν.
U_c For F236 series, velocity of the moving fences. For Couette flows, half the velocity of the moving plate.
U Mean streamwise velocity.
u' Root-mean-square of streamwise velocity fluctuation.
u* Friction velocity.
x Streamwise distance.
y Distance from the fixed wall.
y_s Depth of the sheet of light.
y_w Distance of the hydrogen-bubble wire from the fixed flat plate.
z Spanwise distance.
Δt_{HB} Time interval of successive hydrogen-bubble time lines.
Δx Streamwise length of the vortical streak.
θ Momentum thickness.
λ The spanwise spacing of the vortical streaks or the low-speed streaks.
ν Kinematic viscosity.
$( )^+$ Non-dimensionalized value with u* and ν.
$\overline{( )}$ Mean value.

REFERENCES

Alavyoon, F., Henningson, D. S., and Alfredsson, P. H. (1986), Turbulent Spots in Plane Poiseuille Flow-Flow Visualization, *Phys. Fluids*, vol. 29, no. 4, pp. 1328-1331.

Blackwelder, R. F. and Eckelmann, H. (1979), Streamwise Vortices Associated with the Bursting Phenomenon, *J. Fluid Mech.*, vol. 94, pt. 3, pp. 577-594.

Carlson, D. R., Widnall, S. E., and Peeters, M. F. (1982), A Flow-Visualization Study of Transition in Plane Poiseuille Flow, *J. Fluid Mech.*, vol. 121, pp. 487-505.

Cantwell, B. J. (1981), Organized Motion in Turbulent Flow, *Ann. Rev. Fluid Mech.*, vol. 13, pp. 457-515.

Cantwell, B., Coles, D. and Dimotakis, P. (1978), Structure and Entrainment in the Plane of Symmetry of a Turbulent Spot, *J. Fluid Mech.*, vol. 87, pt. 4, pp. 641-672.

El Telbany, M. M. M. and Reynolds, A. J. (1980), Velocity Distributions in Plane Turbulent Channel Flows, *J. Fluid Mech.*, vol. 100, pt. 1, pp. 1-29.

El Telbany, M. M. M. and Reynolds, A. J. (1982), The Structure of Turbulent Plane Couette Flow, *Trans. ASME: J. Fluids Engng.*, vol. 104, no. 3, pp. 367-372.

Goldsmith, H. L. and Mason, S. G. (1962), Particle Motions in Sheared Suspensions XIII. The Spin and Rotation of Disks, *J. Fluid Mech.*, vol. 12, pt. 1, pp. 88-99.

Hirata, M., Tanaka, H., Kawamura, H., and Kasagi, N. (1982), Heat Transfer in Turbulent Flows, *Proc. 7th Int. Heat Transfer Conf.*, Munich, vol. 1, pp. 31-57.

Iritani, Y., Kasagi, N., and Hirata, M. (1985), Streaky Structure in a Two-Dimensional Turbulent Channel Flow, *Trans. JSME, Ser. B*, vol. 51, no. 470, pp. 3092-3101, in Japanese.

Jeffery, G. B. (1922), The Motion of Ellipsoidal Particles Immersed in a Viscous Fluid, *Proc. R. Soc. Lond., Ser. A*, vol. 102, pp. 161-179.

Kasagi, N., Hirata, M., and Nishino, K. (1986), Streamwise Pseudo-Vortical Structures and Associated Vorticity in the Near-Wall Region of a Wall-Bounded Turbulent Shear Flow, *Exps Fluids*, vol. 4, no. 6, pp. 309-318.

Kreplin, H.-P. and Eckelmann, H. (1979), Propagation of Perturbations in the Viscous Sublayer and Adjacent Wall Region, *J. Fluid Mech.*, vol. 95, pt. 2, pp. 305-322.

Maruyama, S. and Tanaka, H. (1987a), The Effect of Spatial Restriction on the Inner-Layer Structure of Wall Turbulence, *J. Fluid Mech.*, vol. 177, pp. 485-500.

Maruyama, S. and Tanaka, H. (1987b), The Effect of Spatial Restriction on the Inner Layer Structure of Wall Turbulence (2nd Report, The Influence of Streamwise Pitch of the Interfering Plates), *Trans. JSME, Ser. B*, vol. 53, no. 491, pp. 1962-1969, in Japanese.

Nakagawa, H. and Nezu, I. (1981), Structure of Space-Time Correlations of Bursting Phenomena in an Open-Channel Flow, *J. Fluid Mech.*, vol. 104, pp. 1-43.

Savaş, Ö. (1985), On Flow Visualization Using Reflective Flakes, *J. Fluid Mech.*, vol. 152, pp. 235-248.

Smith, C. R. and Metzler, S. P. (1983), The Characteristics of Low-Speed Streaks in the Near-Wall Region of a Turbulent Boundary Layer, *J. Fluid Mech.*, vol. 129, pp. 27-54.

Smith, C. R. and Schwartz, S. P. (1983), Observation of Streamwise Rotation in the Near-Wall Region of a Turbulent Boundary Layer, *Phys. Fluids*, vol. 26, no. 3, pp. 641-652.